PHYSICAL REVIEW D VOLUME 48, NUMBER 11 1 DECEMBER 1993

Rapidity gap signals in Higgs-boson production at the SSC

R. S. Fletcher
Bartol Research Institute, University of Delaware, Newark, Delaware 19716

T. Stelzer
Physics Department, University of Wisconsin–Madison, Madison, Wisconsin 53589
(Received 3 June 1993)

We examine the structure of the underlying event in neutral Higgs-boson production at the Superconducting Super Collider (SSC). Gaps, regions of rapidity containing no soft particle production, can provide a clean signature for W boson fusion to the heavy Higgs boson. We first examine the physical basis of gap production and estimate the survival probability of gaps in the minijet model. Then, using PYTHIA, and HERWIG, we compare gap events to W pair production from top quark decay and $q\bar{q}$ fusion. We find that, if experimental problems can be overcome, gaps should provide a small, but clean, signal for heavy Higgs-boson production at the SSC.

PACS number(s): 13.85.Qk, 13.87.Fh, 14.80.Gt

I. INTRODUCTION

One of the main goals of the Superconducting Super Collider (SSC) is to search for the Higgs particle. The Higgs boson is expected to have a mass in the range from 100 GeV to at most a few TeV. Much study has gone into finding ways of identifying the Higgs particle through its various decay channels [1]. It has been suggested that the structure of the underlying event in Higgs-boson production will differ from normal events, allowing experiments to search for the Higgs boson by looking for events where a "gap" is produced in the central rapidity region [2,3].

There are three components to particle production in high energy hadronic interactions. There are high p_t jets caused by the fragmentation of partons which have undergone a hard scattering. There is an "underlying event" of soft particles which typically has the structure of a minimum bias event, and there are particles generated by the fragmentation of the soft partons radiated from the hard scattering. Although this separation is certainly not unique, it is useful to discuss these components separately when considering the production of rapidity gaps in hadronic interactions.

We have used the minijet model to estimate the survival probability of gaps [3], and find that around 3% of events are free of secondary interactions which would destroy the gap signal. Next we discuss the properties of the underlying event, and of parton radiation in gap events and use the PYTHIA and HERWIG Monte Carlo programs [4–7] to investigate the production of gaps in a full simulation.

II. GAP PRODUCTION AND TAGGING JETS

There are two main, parton level, processes for producing Higgs particles at high energy hadron colliders. First, there is gluon fusion as shown in Fig. 1(a). Here, the Higgs boson is coupled to a pair of gluons through a fermion loop. Because the Higgs boson couples to fermions according to their mass, the term represented by a top quark in the loop dominates the cross section. The cross section grows with the top quark mass because of this coupling, and is large for light Higgs particles, because of the large flux of gluons in the proton. This process dominates Higgs-boson production at the SSC for high top quark masses, or Higgs-boson masses less than around a half a TeV. Second, there is the W-boson fusion reaction, shown in Fig. 1(b). Like resonance production

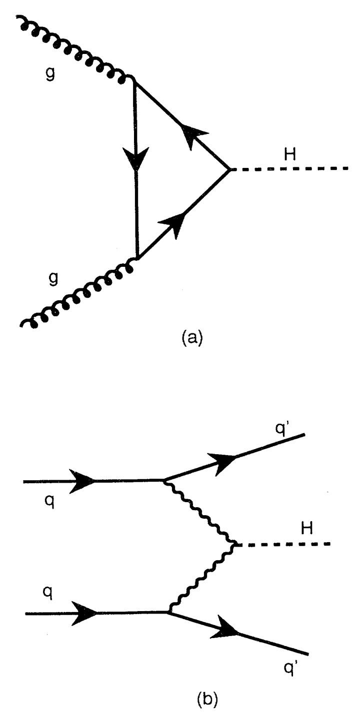

FIG. 1. Higgs-boson production by gluon fusion (a), and by weak boson fusion (b).

in two-photon interactions at e^+e^- colliders, this process can be considered in the effective boson approximation. In this approximation, incoming quarks radiate virtual bosons, here W's. These bosons then collide, and annihilate into a Higgs particle. At the parton level the main property of this process is that the outgoing quarks typically have significant p_t and large energy, and therefore produce jets at large rapidities. This has led to the suggestion of using jet tagging to identify the production of the Higgs boson [8,9]. There is a difference in the color flow in the diagrams shown in Fig. 1. This difference leads to a difference in the underlying event structure in the processes. The W fusion diagram can lead to the production of a "rapidity gap." Gap production occurs when (1) the jets are widely separated and (2) there is *no* particle production in the region between the jets. In a typical high energy event, the region between the jets would be filled with soft particles from the underlying event, and by particles connected with radiation from the hard scattering that produces the jets. In gap production neither component exists, and no particles are produced in the rapidity region between the jets. First we will use a string model for the underlying event to describe how particle production is suppressed in the gap, and then look at parton radiation in the hard scattering.

III. GAP PRODUCTION AND THE UNDERLYING EVENT

To understand how the underlying event is modeled in a string Monte Carlo program, such as PYTHIA, it is easiest to first look at minimum bias events. This is described in detail in Refs. [10,11]. The modeling of minimum bias events in this picture assumes that in a soft hadron reaction the incoming particles exchange color. After interacting, each hadron has broken into two remnants: a quark and a diquark. Two color strings stretch from one forward to one backward remnant. In a proton-proton reaction, each string connects a quark to a diquark forming a color singlet. When these strings fragment, and form particles, they produce an approximately flat rapidity spectrum of mostly mesons, and a pair of leading baryons which carry the original diquarks from the ends of the string. At high energies minijet production changes this simple picture. Typical high energy events contain multiple interactions between the partons [12–14]. Often these interactions are hard enough to add significant transverse momentum to the event, and can be treated perturbatively. These are the minijets. In string models minijets are added to the basic 2-string configuration to account for the increase of average transverse momentum, the p_t-multiplicity correlation, and the excess of events at high multiplicity [15–17].

In typical high p_t events the underlying event is treated in a similar way. For instance, when a two-jet system is formed, the beam particles "lose" a parton to the two-jet system, so the beam fragments carry color. In order to form a color singlet the forward and backward beam fragments must be joined by a string. Again, this fills the central rapidity region with particles. Minijets appear again in the underlying event. Secondary interactions between partons can produce minijets underlying the main, high p_t reaction. Finally, initial-state radiation and final-state showers add more particles to the event.

W-boson fusion events have a different structure. In these events the incoming quarks radiate a color singlet W boson, so the recoiling quark which forms a forward jet, and the surviving beam remnant form a color singlet. Since these partons are both in the forward (backward) region, they will not create particles in the central region. A simple example of this structure is shown in Fig. 2. The figure shows a plot in pseudorapidity η and azimuthal angle ϕ of the particles produced from the fragmentation of two color strings. Each string stretches between a 40 GeV p_t quark jet at pseudorapidity of 4 and a beam remnant moving along the z axis. The plot shows ten SSC events, each with the same parton level configuration, but fragmented separately using the JETSET Monte Carlo program [5]. The gap is clearly evident. Higgs-boson production events will have this structure if the decay products of the Higgs boson can be removed. This configuration is also expected from jet production via the exchange of a neutral boson (W or Z) or Pomeron [18].

When two quarks interact to produce a Higgs boson by W fusion, the remaining clouds of quarks and gluons that form the protons must pass through one another. If there are secondary interactions, either soft color exchange or minijet production, the gap will be destroyed. This leads to a small survival probability for gaps.

The minijet model provides a probabilistic interpretation for parton exchanges [13–15]. When two protons pass through one another at an impact parameter b, the average number of interactions is given by

$$n(b) = \sigma_0 A(b,\mu_1) + \sigma_{\rm jet}\ A(b,\mu_2). \qquad (1)$$

$\sigma_{\rm jet}$ is the cross section for producing hard jets at scales greater than a cutoff $t_{\rm min} = 5.3$ GeV^2, calculated using the proton structure functions of Ref. [19]. $\sigma_0 = 125$ GeV^{-2} is a constant representing softer exchanges, chosen to reproduce the low energy total cross section. $A(b)$ is the overlap function of the two protons in impact parameter space given by

$$A(b,\mu) = \frac{\mu^2}{12\pi}\frac{1}{8}\,(\mu\, b)^3\ \ K_3(\mu\, b),$$
$$\mu_1 = 0.85\ {\rm GeV}, \mu_2 = 0.76\ {\rm GeV}. \quad (2)$$

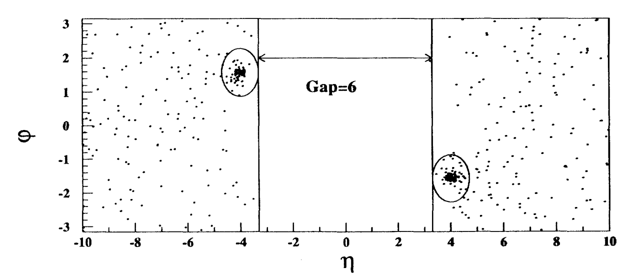

FIG. 2. "Lego plot" for ten superimposed two jet events, with a central gap, modeled with string fragmentation.

Assuming that the interactions are independent, the distribution in the number of interactions is Poissonian, so the probability of having no interactions for impact parameter b is given by $\exp[-n(b)]$. In this model the inelastic and total cross sections are given by [13]

$$\sigma_{\rm inel} = \int d^2b \;\; 1 - e^{-n(b)}, \tag{3}$$

$$\sigma_{\rm tot} = 2 \int d^2b \;\; 1 - e^{-n(b)/2}. \tag{4}$$

If we assume that the distribution of W's in impact parameter space in the proton is the same as for the partons which produce minijets, the inclusive differential cross section in impact parameter space for Higgs-boson production through W fusion is just

$$\frac{d\sigma}{d^2b} = \sigma_{WW \to H} \; A(b, \mu_2) \tag{5}$$

and the cross section for producing a Higgs boson *without* having any secondary interactions is

$$\frac{d\sigma_{\rm gap}}{d^2b} = \sigma_{WW \to H} \; A(b, \mu_2) e^{-n(b)}. \tag{6}$$

The exponential factor suppresses the contribution to the cross section where the two protons overlap and there is likely to be a secondary collision. The integral of Eq. (6), divided by the total production cross section gives a survival probability for the gap. Using these expressions we can calculate the total cross section, elastic slope, and survival probability at different energies. The two values of μ allow the partons contributing to the soft and hard parts of the cross section to have slightly different impact parameter distributions. The value of μ_2, and $t_{\rm min}$ are chosen to fit the values of the total cross section and elastic slope measured at the Fermilab Tevatron [20]: $\sigma_{\rm tot} = 72.1 \pm 3.3$ mb and $B_{\rm el} = 16.5 \pm 0.5$ GeV^{-2}. The results are given in Table I.

In PYTHIA the effect of multiple interactions on the event is explicitly included by producing secondary, low p_t, minijet pairs. We have run separate samples of events with and without multiple interactions. If multiparton interactions in the PYTHIA model [21] are turned on, 96% of events have a secondary interaction which changes the color flow in the event, i.e., PYTHIA predicts a survival probability of 4%, in agreement with our estimate and that of Ref. [3].

TABLE I. Minijet model predictions for scattering parameters and survival probability.

$E_{\rm c.m.}$ [GeV]	$\sigma_{\rm total}$ [mb]	Elastic slope B [GeV^{-2}]	Survival probability (%)
63.0	42	13.3	14
630	58	14.9	10
1800	72	16.0	7.8
40 000	137	21.0	3.3

IV. GAP PRODUCTION AND RADIATION

We have seen that when there is a color singlet exchange between two interacting protons, and there are no secondary interactions, particle production from the underlying event, beam fragmentation, is suppressed, causing a gap. Equally important is the fact that parton, generally gluon, radiation in the region between the tagging jets is also suppressed.

The foundation of all rapidity gap physics is that the structure of an event is dependent on the color structure of the interaction. Since this dependence is so crucial, it is important to understand the physics involved, how this physics is manifest in a perturbative calculation using Feynman diagrams, and how it is implemented in Monte Carlo event simulations. A simple example will be useful in investigating these facets of gap physics. We will consider the $2 \to 2$ process $u + c \to u + c$. There are two possible t channel exchanges between the incoming partons; gluon exchange (QCD) and photon exchange (QED). The Feynman diagrams are shown in Fig. 3.

The difference in the radiation in QED and QCD exchange events can be understood from a simple classical analogy. From electrodynamics, we know that accelerated charges radiate and tend to radiate collinearly. In QCD when a color charge is accelerated, it will result in radiation, primarily tangentially to the path of the accelerated charge. There are 2 relevant angles in the scattering: $\theta_{\rm scatter}$, the angle through which the fermion scatters, and $\theta_{\rm charge}$, the angle through which the color charge scatters. In single gluon or photon exchange, the cross section is large when $\theta_{\rm scatter}$ is small, i.e., small $\hat{t}$. In single photon exchange, $\theta_{\rm scatter} = \theta_{\rm charge}$, the color charge is typically accelerated through angle $\theta_{\rm scatter}$ from the initial direction, and we expect gluon radiation only in the regions collinear to this acceleration; i.e., we only expect radiation when $\theta_{\rm radiation} \lesssim \theta_{\rm scatter}$. Hence there will be a large region of rapidity in which radiation is suppressed.

However for QCD exchange, the *charge* is accelerated from the incoming up quark direction to the outgoing charm quark direction or $\theta_{\rm charge} = 2\pi - \theta_{\rm scatter}$. If we

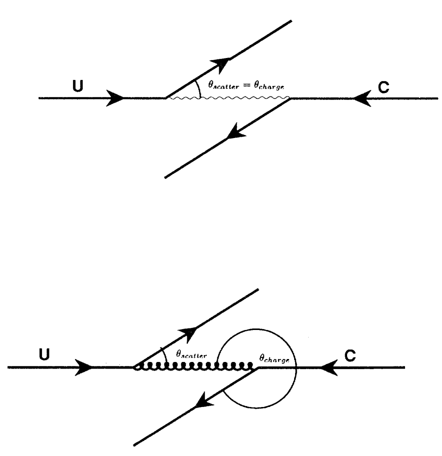

FIG. 3. Graphs for single gluon exchange, and single photon exchange, labeled with color and fermion scattering angles.

follow the classical trajectory of the charge (not fermion), it would be a continuous curve connecting the direction of the incoming up quark to the outgoing charm quark. For small $\theta_{\rm scatter}$ the tangents to this curve cover essentially the entire angular region, so radiation can be produced over the entire rapidity range.

We can see this effect in perturbation theory by calculating the $2 \to 3$ matrix elements [22], and plotting the ratio of the QED to QCD contributions for fixed quark jets, while varying the rapidity of the radiated gluon. The Feynman graphs for the two processes are given by adding an external gluon line to the diagrams in Fig. 3. Figure 4 shows the resulting suppression of radiation in the gap from color singlet (photon) exchange compared with gluon exchange. We fix the final quarks at pseudorapidity, $\eta = \pm 5$ and $p_t = 40$ GeV. The gluon's p_t was fixed at 1 GeV and its rapidity varied from -10 to 10. All three final particles were set in a plane. The quark leg which was furthest from the final-state gluon was given additional p_t to balance the gluon, and the remaining degrees of freedom were used to conserve energy and momentum.

Near the directions of the outgoing fermions, the matrix elements are dominated by initial- and final-state radiation terms, and the photon exchange and gluon exchange matrix elements are similar in shape. This is clear from the excellent cancellation of the singularities in the matrix elements at $\eta_{\rm radiation} = \eta_{\rm jet} = 5$ in Fig. 4. When the radiated gluon is in the central region, far from the outgoing fermions, destructive interference in the photon exchange matrix element suppresses radiation into the gap relative to the gluon exchange process. At high rapidities, beyond the rapidity of the quark jets, destructive interference in the QCD exchange causes a bump in the ratio.

The difference in the radiation in these two processes

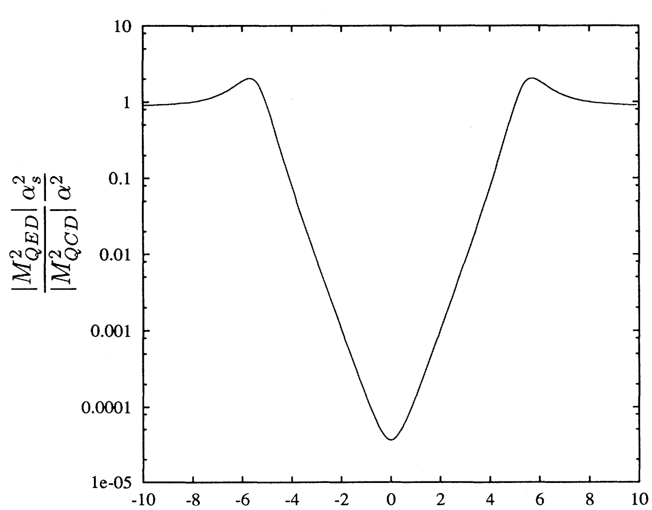

FIG. 4. Ratio of photon vs gluon exchange matrix elements for $qq' \to qq'g$, as a function of the pseudorapidity of the gluon, for quarks fixed at $\eta = \pm 5$, showing the supression of gluon radiation in color singlet exchange.

comes from the different interference between initial- and final-state radiation graphs, and by radiation off the t-channel gluon propagator. In general there is interference between graphs where the gluon is radiated from the same color line. In photon exchange this means that the interference terms come from gluon radiation off a single fermion line. In the gluon exchange case the interference is between radiation off different fermion lines, one initial and one final, or between radiation of a fermion line, and the gluon propagator. These interference terms cause the different radiation patterns.

There is also an interference term between the photon exchange and gluon exchange diagrams when a gluon is radiated off of different fermion lines. This adds a small correction, order $\alpha\alpha_s$, to the nongap forming cross section, which is not included in the figure.

Monte Carlo simulations require a quick method for determining the probability for radiation. They approximate the above interference by using angular ordering. The angular ordering algorithm places a limit on the phase space into which partons can radiate. A cone is drawn around each parton line, whose angle is determined by the angle between that parton, and the parton which is color connected to it in the $1/N_c$ approximation. Radiation in the cone is allowed in the normal leading log approximation. Radiation is not allowed outside the cone. In the production of large gaps, in the small angle approximation, this constraint has a simple form. Radiation is allowed in a cone of half angle $\theta_{\rm charge}$ (see Fig. 3) around the quark jet, or up to an angle $2\theta_{\rm charge}$. In terms of rapidity, radiation is approximately limited by

$$\eta_{\rm max} = -\ln\left[\tan\left(\frac{2\theta_{\rm color}}{2}\right)\right] \tag{7}$$

$$\simeq -\ln\left[\frac{\theta_{\rm color}}{2}\right] - \ln[2] \simeq -\eta_{\rm jet} - 0.7. \tag{8}$$

The angular ordering algorithm replaces the exponential falloff in the central region in Fig. 4 with a cutoff at $\eta \approx 4.3$.

To summarize, radiation is suppressed in the central region when a color singlet is exchanged between partons. This effect can be understood classically, is present in the $2 \to 3$ Feynman amplitudes, and is predicted by the angular ordering algorithm used by the HERWIG Monte Carlo program.

V. HIGGS-BOSON PRODUCTION IN THE HERWIG MONTE CARLO PROGRAM

The angular ordering algorithm used in the HERWIG [6,7] Monte Carlo program includes the color flow information needed to correctly generate parton radiation in gap events. Here we use HERWIG to study the event structure in heavy Higgs-boson production in the processes $WW \to h^0 \to WW$ and $gg \to h^0 \to WW$. We compare these to PYTHIA predictions for $gg \to h^0$, $q\bar{q} \to WW$, and $gg \to t\bar{t} \to WW$. In each case, after generating an event, the W's are eliminated from the event record and excluded from the remaining analysis. We choose $m_h^0 = 500$ GeV and $m_t = 150$ GeV. For the background processes, direct W-pair production and top quark decay to W's, we require the W-pair mass to be between 450 and 500 GeV. We have not done a detailed simulation of the reconstruction of the W's or of other detector acceptances.

Here we do a simple analysis to show the effect of the gap requirement. For each event we count the total multiplicity in the central rapidity range, $\eta < 2$ (charged and neutral $\pi's, k's, \eta's$). Figure 5 shows the HERWIG multiplicity distribution for WW fusion to Higgs boson, and $gg \to h$, and PYTHIA predictions for the backgrounds from direct W pair production and top quark pair decay to W's. The signal from W fusion to the Higgs boson is a peak at multiplicity of zero. 78% of the signal is in the region of multiplicity less than or equal to two. The curves are normalized to the cross section given by HERWIG or PYTHIA, multiplied by the branching ratio squared for the decay of that state to $W+W- \to l^+\nu l^-\bar{\nu}$, and for gap production, by the survival probability of 3%. For WW fusion to Higgs boson this leaves a cross section of 0.72 fb. The total rate for direct W pair production with leptonic decays is 340 fb, but only 0.01% of these have a gap, so the background is small. Top quark decays to W's have a large cross section, and calculating the small fluctuations directly is difficult. The curve in Fig. 5 is a negative binomial fit to the multiplicity distribution from 24 000 events, where the W pair is within 50 GeV of the Higgs-boson mass. The requirement that there be fewer than 2 particles in the central region suppresses the top quark contribution by 6 orders of magnitude, making the background small.

It is important to note that for a Monte Carlo program to give a good description of rapidity gaps, it is neccesary to have a good representation of the effects of interference between initial-state and final-state radiation. We have done tests with the PYTHIA Monte Carlo program, and found that when this interference is not taken into account, the simulation produces many extra particles in the gap region which destroy the gap signal.

A more detailed analysis using jet tagging to define the gap should improve the background rejection, and might help improve the signal by eliminating the long tail on the $WW \to H$ multiplicity distribution. However, it also leads to the rejection of some signal events whose tagging jets are outside the range of detectors. Jet tagging, jet tagging with a gap requirement, and a simple study of the central multiplicity should all be complimentary in an eventual Higgs-boson search.

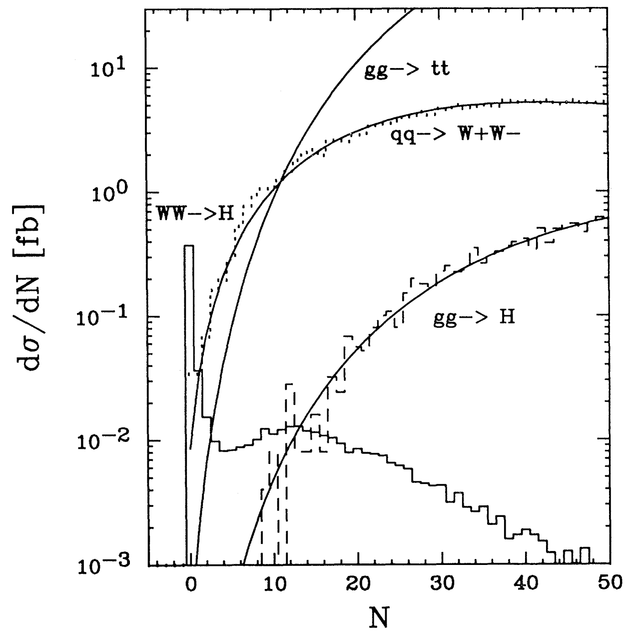

FIG. 5. Multiplicity distributions of particles inside $\eta = 2$ for Higgs-boson production and background processes. Curves are normalized to the cross section times branching ratio to pure leptonic decays of the W.

VI. CONCLUSIONS

Events containing a W boson pair generated by boson-boson fusion at the Higgs-boson resonance at the SSC will have a completely different underlying event structure than other W boson pair events. This difference is caused by the properties of QCD radiation in color singlet exchange processes and by the lack of a soft particle production in the central region. Many events of this type will not "survive" because of spectator parton interactions. We have calculated this survival probability in the minijet model. The survival probability drops at high energies because of the rise of the total and inelastic cross sections. At the SSC about 3% of Higgs-boson production events have no secondary interactions.

In one year at the SSC we expect about 5 events containing a 500 GeV Higgs boson decaying through W's to the "silver plated" mode, electrons, muons, and neutrinos. Requiring that there be a true gap, containing few, or no particles in the central region of the event supresses the background from top quark decays and direct W pair production by 3–6 orders of magnitude. Essentially, there is no background from these processes. It is not necessary to do jet tagging in this case to determine the true edges of the gap.

There are still unresolved problems in making gap production a realistic signal at the SSC. First, experiments must be able to measure soft particle production reliably. Events with as few as 10 soft particles need to be excluded to keep them from overwhelming the gap signal. Second, the experiments must deal with event overlap. A minimum bias event overlapping the Higgs-boson gap event will fill the gap with particles. Unless the tracking is good enough to reliably assign soft particles to the correct vertex, studying gap physics will only be possible at low luminosities when event overlap is small. But the low rate for Higgs-boson production makes this approach impossible unless the total event rate can be increased. This requires that we be able to reconstruct the hadronic decays of the W's, or that our model for the survival probability is wrong. Either of these eventualities might increase the signal rate by an order of magnitude.

ACKNOWLEDGMENTS

We would like to thank Francis Halzen, Dieter Zeppenfeld, J.D. Bjorken, Torbjörn Sjöstrand, V.A. Khoze, and Alan Stange for useful comments. This research was supported in part by the U.S. Department of Energy under Contract No. DE-AC02-76ER00881.

[1] J. Gunion, H. Haber, G. Kane, and S. Dawson, *The Higgs Hunters Guide* (Addison-Wesley, New York, 1990).
[2] Y. L. Dokshitzer, V. Khoze, and T. Sjöstrand, Phys. Lett. B **274**, 116 (1992).
[3] J. D. Bjorken, Phys. Rev. D **47**, 101 (1993).
[4] H. Bengtsson and T. Sjöstrand, Comput. Phys. Commun. **46**, 43 (1987).
[5] T. Sjöstrand and M. Bengtsson, Comput. Phys. Commun. **43**, 367 (1987).
[6] G. Marchesini *et al.*, Comput. Phys. Commun. **67**, 465 (1992).
[7] G. Marchesini and B.R. Webber, Nucl. Phys. **B310**, 461 (1988).
[8] R. Cahn, Phys. Rev. D **35**, 1626 (1987).
[9] V. Barger, K. Cheung, T. Han, and D. Zeppenfeld, Phys. Rev. D **44**, 2701 (1991).
[10] A. Capella and J. Tran Thanh Van, Z. Phys. C **10**, 249 (1981).
[11] T. Sjöstrand and M. van Zijl, Phys. Rev. **36**, 2019 (1987).
[12] P. L'Heureux, B. Margolis, and P. Valin, Phys. Rev. D **32**, 1681 (1985).
[13] L. Durand and H. Pi, Phys. Rev. Lett. **58**, 303 (1987); Phys. Rev. D **38**, 78 (1988); **40**, 1436 (1989).
[14] M. Block, R.S. Fletcher, F. Halzen, B. Margolis, and P. Valin, Phys. Rev. D **41**, 978 (1990).
[15] T. K. Gaisser and T. Stanev, Phys. Lett. B **219**, 375 (1989).
[16] X.-N. Wang, Phys. Rev. D **43**, 104 (1991).
[17] R. S. Fletcher, T.K. Gaisser, T. Stanev, and P. Lipari, in *Proceedings of the 22nd International Cosmic Ray Conference*, Dublin, Ireland, 1991, edited by M. Cawley *et al.*, (Dublin Institute for Advanced Studies, Dublin, 1992).
[18] H. Chehime *et al.*, Phys. Lett. B **286**, 397 (1992).
[19] D. W. Duke and J. F. Owens, Phys. Rev. D **30**, 49 (1984).
[20] E710 Collaboration *et al.*, Phys. Lett. B **243** (1990).
[21] T. Sjöstrand and M. van Zijl, Phys. Lett. B **188**, 149 (1987).
[22] R.K.Ellis, G. Marchesini, and B.R. Webber, Nucl. Phys. **B286**, 643 (1987).
[23] M. Bengtsson and T. Sjöstrand, Nucl. Phys. **B289**, 810 (1987).